# Seismic energy radiation and along-strike heterogeneities of shallow tectonic tremors at the Nankai Trough and Japan Trench

**Suguru Yabe[1]*, Satoru Baba[2], Takashi Tonegawa[3], Masaru Nakano[3], Shunsuke Takemura[2]**

[1]Geological Survey of Japan, National Institute of Advanced Industrial Science and Technology (AIST), Tsukuba Central 7, 1-1-1 Higashi, Tsukuba, Ibaraki, 305-8567, Japan

[2] Earthquake Research Institute, the University of Tokyo, 1-1-1, Yayoi, Bunkyo, Tokyo, 113-0032, Japan

[3] Japan Agency for Marine-Earth Science and Technology (JAMSTEC), 3173-25, Showa-machi, Kanazawa, Yokohama, Kanagawa, 236-0001, Japan

Corresponding author: Suguru Yabe (s.yabe@aist.go.jp)

**Highlights:**

- Shallow tremor seismic energy rates exhibit significant along-strike variations.
- Tremors with higher energy rates tend to have longer recurrence intervals.
- Shore-based monitoring could underestimate shallow slow earthquake activity.

**Abstract**

Shallow slow earthquakes have been documented along shallow plate interfaces near trenches. Recent geophysical observation networks located offshore of Japan enable us to analyze shallow tremors in the Nankai Trough and the Japan Trench. Onshore seismic stations are also important for detecting shallow very low frequency earthquakes (VLFEs) and for evaluating their seismicity prior to the deployment of offshore observation networks. This study analyzes data from ocean bottom seismometers to estimate the seismic energy radiation of such tremors, from which we observe along-strike heterogeneity. Tremors with higher seismic energy rates tend to have longer recurrence intervals, which has also been observed for deep tremors. This study also estimates seismic moment releases of shallow VLFEs at the Japan Trench observed by onshore seismic stations using Green's function in a local three-dimensional seismic velocity model. The scaled energy, which is the ratio of the seismic energy (rate) to the seismic moment (rate), is ~$10^{-9}$. Shallow slow earthquakes located off the Kii Peninsula and Cape Muroto in the Nankai Trough have higher values ($10^{-9}$–$10^{-8}$), while shallow slow earthquakes located off the Kii channel in the Nankai Trough and in the Japan Trench have lower values ($10^{-10}$–$10^{-9}$), which are similar to the values estimated for deep slow earthquakes. By comparing the cumulative seismic energy of the shallow tremors with the cumulative seismic moment of shallow VLFEs, we evaluate the monitoring of shallow tremors and shallow VLFEs in the Japan Trench, suggesting that monitoring shallow VLFEs based on data from onshore seismic stations could miss many (~90% at most) of the seismic moment releases by small magnitude but frequent events.

**Keywords:** slow earthquake, shallow tremor, very low frequency earthquake, Nankai Trough, Japan Trench

# 1. Introduction[1]

Plate boundary faults at subduction zones host slow earthquakes, as well as megathrust earthquakes. Slow earthquakes have been detected since the beginning of the 21st century owing to the development of dense seismic and geodetic observation networks (e.g., Beroza and Ide, 2011; Obara, 2011). Slow earthquakes were first documented in subduction zones in southwestern Japan and in Cascadia along the deep plate interface (30-40 km). Continuous seismic signals have been detected in southwestern Japan at 2–8 Hz and are known as tectonic tremors (Obara, 2002). Seismic signals of 0.01–0.1 Hz have also been detected in southwestern Japan, which are known as very low frequency earthquakes (VLFEs) (Obara and Ito, 2005). Slow deformation signals have also been observed in geodetic data at the Cascadia subduction zone, which are known as slow slip events (SSEs) (Dragert et al., 2001). These episodic tremors and slips (ETSs) are spatiotemporally correlated and occur repeatedly (Rogers and Dragert, 2003; Obara et al., 2004; Ito et al., 2007). Although microseisms excited by oceanic phenomena (e.g., Longuet-Higgins, 1950; Hasselmann, 1963) often divide tremor and VLFE signals, slow earthquake signals have been detected in the frequency band of microseisms as well when microseisms are quiet (Kaneko et al., 2018) or when the signal-to-noise ratio is improved using the stacking technique (Masuda et al., 2020). This suggests that slow earthquakes are broadband phenomena, and that tremors, VLFEs, and SSEs represent the same slip observed in different frequency bands (Ide and Maury, 2018).

Slow earthquakes have been detected recently along the shallow plate interface (~10 km) near the trench. Shallow VLFEs were initially detected by onshore broadband seismic stations (Obara and Ito, 2005; Asano et al., 2008; Ito et al., 2009; Matsuzawa et al., 2015). Observational networks have been deployed in offshore regions around Japan (Aoi et al., 2020), following these initial observations. Onshore observational data are still important for understanding the long-period seismicity of shallow slow earthquakes (Takemura et al., 2019; Baba et al., 2020a) because the observational period of the offshore data is still short. However, offshore observational instruments reveal detailed characteristics of the shallow slow earthquakes. The Dense Oceanfloor Network system for Earthquakes and Tsunamis (DONET) has been deployed along the Nankai Trough (Figure 1a) (Kaneda et al., 2015; Kawaguchi et al.,

[1] DONET – Dense Oceanfloor Network system for Earthquakes and Tsunamis; ETS – episodic tremors and slips; OBS – ocean bottom seismometer; S-net – Seafloor Observation Network for Earthquakes and Tsunamis; SSE – slow slip event; VLFE – very low frequency earthquake

2015). Shallow tectonic tremors and VLFEs were subsequently detected at 5–10 km depths using the broadband ocean bottom seismometers (OBSs) connected to DONET (Araki et al., 2017; Nakano et al., 2016, 2018). Shallow slow slips have also been documented using a pressure gauge deployed in a borehole in the Nankai Trough (Araki et al., 2017). Shallow slow earthquakes in the Nankai Trough selectively occur in weakly coupled regions (Baba et al., 2020b). In the Japan Trench (Figure 1b), the Seafloor Observation Network for Earthquakes and Tsunamis (S-net) has been deployed. Shallow tectonic tremors have been documented at ~10–20 km depths using short-period OBSs connected to S-net (Nishikawa et al., 2019; Tanaka et al., 2019). Tectonic tremors have not been detected within the large slip zone of the Tohoku-oki earthquake by S-net, although tremors and SSEs were reported prior to the Tohoku-oki earthquake within the large slip area (Ito et al., 2013; 2015). Regular earthquakes occur around the slow earthquake source area, which differs from the along-dip separation observed in the Nankai Trough (Nishikawa et al., 2019).

Slow earthquake activity can be quantified in terms of seismic energy rate, seismic moment rate, and scaled energy. The seismic energy rate measures the size of the tectonic tremor, whereas the seismic moment rate measures the size of the VLFE. The scaled energy is the ratio of the seismic energy (rate) to the seismic moment (rate). The seismic energy rates and cumulative seismic energies of deep tectonic tremors are known to vary widely in space (Maeda & Obara, 2009; Yabe & Ide, 2014; Annoura et al., 2016). Along-dip variations in seismic energy rate have been observed in the Nankai Trough and the Cascadia margin, such that shallower tremor zones tend to have larger seismic energy rates (Yabe and Ide, 2014). Tremor recurrence intervals vary correspondingly, such that the shallower tremor zones have longer recurrence intervals (Wech and Creager, 2011; Idehara et al., 2014). Along-strike variations are observed to correlate with SSE slip distributions (Yabe & Ide, 2014; Annoura et al., 2016). The scaled energy of deep slow earthquakes at several subduction zones is known to be $10^{-10}$–$10^{-9}$ (Ide & Yabe, 2014; Ide, 2016; Maury et al., 2016, 2018), which is much smaller than values estimated for regular earthquakes (approximately $10^{-5}$) over a wide range of seismic moments (Ide and Beroza, 2001). Yabe et al. (2019) estimated the seismic energy rate of shallow tectonic tremors beneath the DONET1 sites, which are located off the Kii Peninsula in southwestern Japan. The scaled energy of shallow slow earthquakes in the DONET1 region is estimated to be approximately $10^{-9}$–$10^{-8}$, which is slightly higher than values estimated for deep slow earthquakes. They also found that the estimated seismic energy rate exhibits along-dip variations that are similar to those of the deep slow earthquakes. However, along-strike variations were not documented because the investigated tectonic tremors were all distributed in one cluster.

This study expands the analyses of seismic energy rates of shallow tectonic tremors and seismic moment rates of the accompanying shallow VLFEs to events throughout the entire Nankai Trough and Japan Trench, and also evaluates the along-strike variations. We estimate the seismic energy rates of shallow tremors following the procedure of Yabe et al. (2019) using data obtained from DONET and S-net. This method is composed of three steps: site amplification estimation, seismic attenuation estimation, and seismic energy rate estimation. We also discuss the observed along-strike variations in estimated seismic energy rates and the differences between slow earthquake monitoring by measuring shallow VLFEs using onshore broadband stations and by measuring shallow tremors using OBSs.

## 2. Data & Methods

### 2.1. Slow earthquake catalogs and seismic data

We estimated the seismic energy rates of shallow tremors and the seismic moment rates of VLFEs based on slow earthquake catalogs published by previous studies (Nakano et al., 2016, 2018; Nishikawa et al., 2019). As slow earthquakes are broadband phenomena (Ide and Maury, 2018), we assumed that seismic signals of tremors and VLFEs are observed simultaneously (Ide and Yabe, 2014; Ide, 2016; Maury et al., 2018). In the Nankai Trough, we used the VLFE catalog of Nakano et al. (2016, 2018) (Figure 1a). As tremors in the DONET1 region were already analyzed by Yabe et al. (2019), tremors in the DONET2 region only are analyzed in this study. The VLFE catalog of Nakano et al. (2016, 2018) extends from August 2015 to April 2016. To estimate the seismic energies of shallow tremors, we used seismic data obtained from the broadband DONET2 stations (National Research Institute for Earth Science and Disaster Resilience, 2019a). In order to estimate the site amplification factors for the DONET2 stations, we also used data from the onshore Hi-net (National Research Institute for Earth Science and Disaster Resilience, 2019b) and F-net (National Research Institute for Earth Science and Disaster Resilience, 2019c) stations. The seismic moment rates were calculated using the seismic moments and durations of the VLFEs listed in the catalog. In the Japan Trench, we used the tremor catalog of Nishikawa et al. (2019) (Figure 1b), which extends from August 2016 to August 2018. We estimated the seismic energy rates of the tremors using short-period records obtained from S-net stations (National Research Institute for Earth Science and Disaster Resilience, 2019d) that were corrected for instrumental responses and sensor orientations (Takagi et al., 2019). The seismic moment rates of the VLFEs were also estimated using broadband records obtained from onshore F-net stations. We also used data from the F-net stations to estimate the site amplification factors of the S-net stations.

2.2. Seismic energy rate estimation for shallow tremors.

The seismic energy rates of tremors were estimated following the procedure of Yabe et al. (2019), with minor modifications for adjusting to the different seismic networks. This method is composed of three steps: estimating the site amplification factors for OBSs, estimating the seismic attenuation, and estimating the seismic energy rate. Site amplification factors are estimated using seismic signals from intra-slab earthquakes. The seismic attenuation and seismic energy rates are estimated using seismic signals from tectonic tremors. These analyses were conducted after applying a 2–8 Hz bandpass filter to the seismic data. As a detailed description of the method is presented in Yabe et al. (2019), here we present a brief description of the procedure.

In the first step, site amplification at each of the OBS sites was evaluated. OBSs are placed on soft sediments and the amplitudes of seismic waves observed at these stations are amplified compared to onshore stations. We measured the maximum S-wave amplitudes of intra-slab earthquakes deeper than 40 km and larger than magnitude 3.0 in the Nankai Trough and 3.5 in the Japan Trench for the OBSs and onshore stations (F-net and Hi-net in the Nankai Trough and F-net in the Japan Trench) (Figure 1). Intra-slab earthquakes were chosen from the Japan Meteorological Agency (JMA) earthquake catalog in the area shown in Figure 1 for the period of January 2015–June 2018 in the Nankai Trough and September 2016–December 2018 in the Japan Trench. We corrected for geometric spreading by multiplying by $4\pi R^2$, where $R$ is the hypocentral distance calculated using the hypocentral locations of the earthquakes in the JMA catalog. The parameters for seismic attenuation and the site amplification factors were inverted from the measured S-wave amplitudes. In the Nankai Trough, site N.KMTF was set as a reference station, for which the site amplification factor was assumed to be 2, including the free surface effect as analyzed for DONET1 by Yabe et al. (2019). In the Japan Trench, the average site factor values of the 11 F-net stations were also assumed to be 2. Relative differences in site amplification for the F-net stations are usually less than a few dB (Takemoto et al., 2012).

In the second step, seismic attenuation parameters that represent the attenuation strength averaged from the shallow plate boundary fault (where slow earthquakes occur) to the OBSs were estimated as a function of the hypocentral distances. As high-frequency seismic waves are attenuated by seismic scattering or intrinsic attenuation, a correction for seismic attenuation is required to accurately estimate the seismic energy (Ide and Beroza, 2001). We first defined time windows in which seismic signals of shallow tremors were observed. In the Nankai Trough, each time windows began at the origin time of the VLFE in the Nakano et al. (2016, 2018) catalog and spanned 100 s. In the Japan Trench, each time window began 100 s before the calculated arrival time of the tremor and spanned 200 s. Tremor arrival times were calculated by adding the travel time of the seismic waves to the origin time in the Nishikawa et al. (2019) tremor catalog, assuming an S-wave velocity of 2 km/s. For each OBS, we calculated the cross-correlation functions of the envelope waveforms with other nearby OBSs that were closer than 100 km. In the Nankai Trough, data were not used for further analyses if the maximum values of the cross-correlation coefficients did not exceed 0.6 for any station pair. In the Japan Trench, data were not used for further analyses if fewer than three station pairs had maximum cross-correlation coefficients that exceeded 0.5. We normalized the envelope waveforms of the shallow tremors and stacked them for stations with tremor signals. We defined the durations of the shallow tremors using the half-value width of the stacked envelope waveforms. We calculated the seismic energy within the tremor duration ($E_{ij}$) observed for the *i*-th tremor and *j*-th OBS, assuming a crustal density of 2700 kg/m$^3$ and a shear wave velocity of 3.5 km/s (Maeda and Obara, 2009). $E_{ij}$ is expressed as:

$$\log(E_{ij}) = \log(E_i) - \log\left(4\pi R_{ij}^2\right) - 2C(R_{ij})R_{ij}, \qquad (1)$$

where $C(R_{ij})$ is a seismic attenuation parameter treated as a step function of the hypocentral distance $R_{ij}$ with 20 km increments. By calculating the differences in Equation 1 for the same tremor at different stations, the seismic energy at the source $E_i$ is canceled out. Then, the seismic attenuation parameter can be estimated by solving the least-squares inversion problem.

In the third step, $E_i$ was estimated by calculating the logarithmic average of the seismic energies observed at the OBSs, corrected for geometric spreading and seismic attenuation. The seismic energy rate was then calculated by dividing the estimated $E_i$ by the duration of the tremors defined above.

Takemura et al. (2020) showed that the estimated durations of shallow tremors described above could be overestimated. An accretionary prism with a low seismic velocity is present in the Nankai Trough. This contributes to the energy trapping of seismic waves and the elongation of seismic wave pulses observed by the OBSs. This is especially effective for seismic sources located just beneath the low-velocity accretionary prism, such as shallow slow earthquakes in the Nankai Trough. However, the method used in this study was selected to allow for consistent comparisons of the estimated results with those of Yabe et al. (2019) in the DONET1 region. Tremor signals would not be elongated significantly in the Japan Trench, where the shallow prism is composed of a Cretaceous backstop that has been imaged as a high-velocity body (Tsuru et al., 2000, 2002). Developing a more precise estimation method should be addressed in future research.

### 2.3. Seismic moment rate estimation for shallow VLFEs.

Seismic moment rates of shallow VLFEs that accompany shallow tremors were estimated by comparing the synthetic VLFE waveforms with the observed waveforms in a frequency band of 0.02–0.05 Hz using three-component seismograms from 10 F-net stations located close to the hypocenter of the VLFEs (Baba et al., 2020a). Synthetic VLFEs were calculated with OpenSWPC (Maeda et al., 2017) using the three-dimensional seismic velocity structure from the Japan Integrated Velocity Structure Model (Koketsu et al., 2012), the seismic moment tensor from the subducting plate model (Nakajima & Hasegawa, 2006; Nakajima et al., 2009; Kita et al., 2010), and the NUVEL-1A plate motion model (DeMets et al., 1994). We set the grids along the average locations of the tremors (Figure 1b). The hypocentral locations of the VLFEs are assumed to be located in the closest grids to the tremor hypocentral locations. This approximation is required to reduce the calculation costs of the synthetic VLFE waveforms. We assumed a triangular shape for the seismic moment rate function. The durations and origin times of the VLFEs were investigated using a grid search. In the grid search, the durations were considered to be between 10 and 50 s, as in Takemura et al. (2019). Origin times were considered to be between 30 s before and 30 s after the origin times of the tremors in the catalog. The parameter set that produces the highest values of the average cross-correlation coefficient among the stations and components between the observed and synthetic waveforms was then adopted. Seismic moments were estimated by fitting the observed waveforms to the synthetic ones based on the variance reduction (e.g., Baba et al., 2020b). To discard bad estimations due to low signal to noise ratios, we excluded results with average cross correlation coefficients less than 0.25. This threshold is comparable to the threshold of VLFE detection using the matched filter technique of Baba et al. (2020a). As the VLFE catalog of Nakano et al. (2016, 2018) already includes information on the seismic moment rates, we applied this method only to the Japan Trench.

## 3. Results

### 3.1. Site amplification factors

The site amplification factors of the DONET2 stations were estimated relative to the onshore F-net N.KMTF station, which was assumed to have a site amplification factor of 2 (Figure 2). We observed strong amplification of the horizontal components, whereas the vertical components were not generally amplified significantly. This tendency is similar to the results for the DONET1 stations (Yabe et al., 2019; Figure 2). The site amplification factors of the S-net stations were estimated relative to the average site factors of 11 onshore F-net stations (Figure 3). The S-net stations also show the tendency for significant amplification of the horizontal components, whereas the vertical components were less amplified. As demonstrated by the numerical simulations of Li et al. (2015), strong shear wave velocity reductions in soft sediments at the seafloor cause significant amplification of horizontal components. The S-net stations also exhibit a spatial trend in which deeper OBSs near the trench have higher site amplification factors in both the horizontal and vertical components. Although we do not go into details on this topic in this study, spatial variations in the thickness of the soft sediment could be related to the observed spatial variations in the site amplification factor.

### 3.2. Seismic attenuation

Seismic attenuation was estimated as a step function with 20 km increments (Figure 4). The estimated seismic attenuation at DONET2 and S-net stations had values of approximately 0.02 $km^{-1}$, which is similar to the values estimated for the DONET1 stations (Yabe et al., 2019; Figure 4). In contrast, seismic attenuation estimated from deep tremors had values of approximately 0.01 $km^{-1}$ (Yabe & Ide, 2014). As discussed in Yabe et al. (2019), differences in the estimated seismic attenuation can be explained by differences in the shear wave velocity structure of the crust through which the seismic waves of tectonic tremors pass. The seismic attenuation parameter $C$ can be written as $\pi f/Q\beta$, where $f$ is frequency, $Q$ is the quality factor, and $\beta$ is the shear wave velocity, all of which are averaged over the ray path from the source to stations. Seismic waves from deep tremors radiate from a depth of ~30 km and pass through the entire southwestern Japan island arc crustal section. Island arc crust has a shear wave velocity of ~4 km/s near the depth of the plate interface and ~3 km/s at the surface (Hirose et al., 2008). In contrast, seismic waves from shallow tremors radiate from depths of ~5–10 km in the Nankai Trough and ~10 km in the Japan Trench. The accretionary prism in the Nankai Trough has a shear wave velocity of ~2 km/s near the plate interface and <1 km/s at the seafloor (Tonegawa et al., 2017). The shallow prism in the Japan Trench has a shear wave velocity of ~3.0–3.5 km/s near the plate interface (Yamamoto et al., 2013). The shear wave velocity of the prism at the seafloor was estimated by laboratory experiments on core samples recovered by scientific drilling and is ~1 km/s (Nakamura et al., 2014). Therefore, path-averaged shear wave velocities could be 2–3 times different for deep and shallow tremors, which can explain the differences in the estimated seismic attenuation parameter $C$.

### 3.3. Seismic energy and seismic moment rates of slow earthquakes in the Nankai Trough

Shallow tremors were distributed as two clusters in the DONET2 region (Figure 1a). The eastern and western clusters were located off the Kii channel and off Cape Muroto, respectively. The estimated seismic energy and moment rates are summarized in Figure 5. The estimated seismic energy rate ranged from $10^3$ to $10^{4.5}$ J/s for both the eastern and western clusters. The seismic moment rates obtained by Nakano et al. (2016, 2018) ranged from $10^{13}$ to $10^{14}$ Nm/s for the eastern cluster and from $10^{12}$ to $10^{13}$ Nm/s for the western cluster. The calculated scaled energy ranged from $10^{-10}$ to $10^{-9}$ for the eastern cluster and from $10^{-9}$ to $10^{-8}$ for the western cluster.

Spatial variations in the estimated seismic energy rate, seismic moment rate, and scaled energy are presented in Figure 6. In the DONET1 region, as discussed in Yabe et al. (2019), along-dip variations in the seismic energy rate and the seismic moment rate were observed. In contrast, such along-dip variations were not observed in the DONET2 region because the cluster size was so small that along-dip variations could not be resolved.

### 3.4. Seismic energy and seismic moment rates of slow earthquakes in the Japan Trench

Shallow tremors in the Japan Trench were grouped into 4 regions: regions off Tokachi, off Iwate, off Fukushima, and off Ibaraki, from north to south (Figure 1b). The seismic energy rates of tremors off the Tokachi region ranged from $10^2$ to $10^5$ J/s. The seismic moment rate in this region spans between $10^{12.5}$ and $10^{14}$ Nm/s (Figure 7). The maximum seismic energy rates of the tremors in the region off Iwate ($10^4$ J/s) are smaller than those in the region off Tokachi. Tremors in the regions off Fukushima, Iwate, and Ibaraki exhibit similar seismic energy rates and seismic moment rates. The calculated scaled energy in all regions ranged from $10^{-10}$ to $10^{-9}$.

Spatial variations in the estimated seismic energy rate, seismic moment rate, and scaled energy are presented in Figure 8. Figure 8a shows that the seismic energy rate varies significantly along strike. Figure 8b shows that VLFEs were detected only at locations where large tremors also occurred. For example, many VLFEs were detected in the region off Tokachi, where large tremors also occurred. On the other hand, the region off Iwate, which is distinguished from the region off Tokachi by a small tremor gap at 40.7°N, exhibited a smaller seismic energy rate and fewer VLFEs were detected. Few VLFEs were detected in the regions off Fukushima and Ibaraki, where the seismic energy rates of the tremors were also lower. VLFEs may occur at locations where smaller tremors occur, although they are difficult to detect using onshore F-net stations due to their low signal-to-noise ratios.

## 4. Discussion

### 4.1. Spatial variations in estimated source parameters of shallow slow earthquakes

Shallow tremors in the DONET2 region in the Nankai Trough were distributed in two clusters (Figure 6). Shallow tremors in the two clusters had similar seismic energy rates, whereas the accompanying shallow VLFEs in the eastern cluster had larger moment rates than those in the western cluster, resulting in smaller scaled energies in the eastern cluster. The scaled energies of the western cluster ($10^{-9}$–$10^{-8}$) are similar to those of shallow slow earthquakes in the DONET1 region (Yabe et al., 2019), whereas the scaled energies of the eastern cluster ($10^{-10}$–$10^{-9}$) are similar to those of deep slow earthquakes (Ide and Yabe, 2014; Ide, 2016; Maury et al., 2018).

Tonegawa et al. (2017) estimated the shear wave velocity structure beneath the DONET stations by analyzing the Rayleigh admittance. They found that low-velocity anomalies are localized in regions where shallow slow earthquakes have been detected, which is interpreted as the presence of fluid contributing to the occurrence of slow earthquakes. This low-velocity anomaly is especially strong in the western cluster in the DONET2 region compared to other slow earthquake source regions in the Nankai Trough, although the source parameters of the western cluster are similar to those in the DONET1 region and are different from those in the eastern cluster in the DONET2 region. Although the presence of elevated fluid pressures has been noted as important for the seismogenesis of slow earthquakes since the initial stages of slow earthquake research (e.g., Obara, 2002), other physical conditions along the plate interface might also be important for determining the seismicity of slow earthquakes.

Ike et al. (2008) investigated spatial variations in the thicknesses of incoming sediments on the Philippine Sea plate. Sediment thickness at the trench (Fig 4 of Ike et al., 2008) correlates with the spatial distribution of slow earthquakes in that the sediment is thicker in regions where shallow slow earthquakes occur along the plate interface. Sediments are especially thick in the eastern cluster in the DONET2 region, which have lower scaled energies than the other cluster. Since geologic records of slow earthquakes have been reported in the viscous shear zone in the subduction mélange (Ujiie et al., 2018; Phillips et al., 2020), lithological differences could be another important factor in slow earthquake occurrence.

Shallow tremors in the Japan trench exhibit band-like distributions (Figure 8) as do deep tremors in southwestern Japan and Cascadia, although the seismicity exhibits strong along-strike variations (Nishikawa et al., 2019; Tanaka et al. 2019). For example, recurrence patterns differ among the studied regions (Figure 9). Shallow tremors in the region off Tokachi have long recurrence intervals (~0.5–1 year), while shallow tremors in the region off Iwate have short recurrence intervals (1–2 months). Shallow tremors in the regions off Fukushima and Ibaraki have medium recurrence intervals (~3 months). Our results show that the estimated seismic energy rates also differ correspondingly among the four regions (Table 1). The region off Tokachi has the longest recurrence interval and the largest seismic energy rate (median rate of 1700 J/s), whereas the region off-Iwate has the shortest recurrence interval and the lowest seismic energy rate (830 J/s). The regions off Fukushima and Ibaraki have medium recurrence intervals and medium energy rates (1350 and 1470 J/s, respectively). This correlation between energy rate and recurrence interval has also been observed for deep slow earthquakes. Recurrence intervals in southern Cascadia (44–47°N) are longer than those in northern Cascadia (47–50°N) (Brudzinski and Allen, 2007). The estimated seismic energy rate is also higher in southern Cascadia (Yabe and Ide, 2014). The same correlation has also been observed in the along-dip direction. Up-dip tremors in deep slow earthquakes tend to have larger energy rates (Yabe and Ide, 2014) and longer recurrence intervals (Wech and Creager, 2011; Idehara et al., 2014). As the energy rates of tremors could represent stress drops (Ando et al., 2012), this correlation may result from the fact that tremor zones with higher frictional strengths can endure larger stress loading. The estimated scaled energy range for the shallow slow earthquakes throughout the Japan Trench ($10^{-10}$–$10^{-9}$) is similar to that of the eastern cluster in the DONET2 region and that of deep slow earthquakes.

Shallow tremors in the regions off Tokachi and Iwate are separated by a small gap at 40.7°N. Tanaka et al. (2019) noted that aftershocks of the 1994 Sanriku-oki earthquake (Mw 7.7; Nagai et al., 2001) were located in this gap. This suggests that the physical conditions along the plate interface change across this area. The seismic structure of the shallow accretionary prism along the Japan Trench has been investigated using seismic reflection surveys (e.g., Tsuru et al., 2000, 2002; Kodaira et al., 2017; Azuma et al., 2018) and is composed of a Cretaceous backstop and a deformed prism toe (Tsuru et al., 2000), although the size and shape of the deformed prism toe vary along strike (Tsuru et al., 2002; Kodaira et al., 2017; Azuma et al., 2018). The deformed prism toe has a wedge shape in the northern Japan Trench, whereas prism toe sediments are subducted as thin channel-like layers in the southern Japan Trench (Tsuru et al., 2002). This transition occurs abruptly at 37.5°N (Kodaira et al., 2017). The size of the wedge-shaped prism toe is estimated to be small in the large slip zone of the 2011 Tohoku-oki earthquake located at 38–39° N, whereas the size of the prism toe increases in the northern region (Azuma et al., 2018).

Almost no tremors were detected in the large slip area of the Tohoku-oki earthquake in the Nishikawa et al. (2019) tremor catalog. Shallow VLFE activity, which is monitored by onshore seismic stations, has also been limited in this region (Matsuzawa et al., 2015; Baba et al., 2020a), which suggests that shallow slow earthquakes are not active in this region. This could be related to the small size of the deformed prism toe in this region. Underthrust sediment in the deformed prism toe has been imaged as a low-velocity layer (Tsuru et al., 2000, 2002), which suggests that the prism toe sediment transports fluid to depth. In regions where the deformed prism toe is small, sufficient fluid cannot be transported to the depth where shallow slow earthquakes occur, which hinders the occurrence of shallow slow earthquakes. In the regions off Iwate and Tokachi where the deformed prism toe is sufficiently large, the low-velocity sediments have been imaged to a depth of 10–15 km (Tsuru et al., 2002), which could produce favorable physical conditions for shallow slow earthquakes. However, no abrupt changes in seismic structure profiles have been reported across the tremor gap at 40.7°N.

In the southern Japan Trench, prism toe sediments have been imaged as a thin low-velocity layer that extends to a depth of 10–20 km (Tsuru et al., 2002). This may also contribute to the generation of favorable physical conditions for shallow slow earthquakes in the regions off Fukushima and Ibaraki with high pore fluid pressures.

Fujie et al. (2020) investigated the spatial variations in the incoming sediments on the Pacific plate. Although their results for the trench cover only shallow tremors in the region off Iwate, we can observe spatial correlations between the sediment thickness and slow earthquakes. The southern edge of the tremor zone corresponds to the thin-sediment region due to petit-spot volcanism (Hirano et al., 2006). The northern edge of the tremor zone off Iwate seems to correspond to a region of thick sediments, although it is unfortunately located at the edge of the area analyzed by Fujie et al. (2020). Similar to the Nankai Trough, lithological differences may affect the seismicity of slow earthquakes.

### 4.2. Shallow slow earthquake monitoring using tremors and VLFEs

As slow earthquakes frequently release strain aseismically, it is important to monitor slow earthquake activity to understand strain accumulation in the locked zone of future megathrust earthquakes (e.g., Obara and Kato, 2016). As frequent geodetic measurements are difficult in offshore areas (e.g., Yokota et al., 2016), shallow tremors and VLFEs are important monitoring targets. Seismic signals of shallow tremors are not usually observed by onshore seismic stations, offshore seismic networks (such as DONET and S-net) are required to conduct real-time monitoring. In contrast, seismic signals of shallow VLFEs are observed by onshore broadband seismic stations (Asano et al., 2008; Matsuzawa et al., 2015; Takemura et al., 2019; Baba et al., 2020a).

Baba et al. (2020b) estimated the seismic moment release rates of VLFEs in the Nankai Trough and the Japan Trench. In the Japan Trench, VLFE activity in the region off Tokachi had higher estimated moment release rates ($10^{6.5}$–$10^{7.5}$ N/m/yr) than in other regions ($10^{5.0}$–$10^{6.0}$, ~$10^{5.5}$, and $10^{5.5}$–$10^{6.5}$ N/m/yr in the regions off Iwate, Fukushima, and Ibaraki, respectively). Figure 9a and 9b show time plots of the cumulative moment released by shallow VLFEs estimated in this study. Although the analytical period differs between this study and that of Baba et al. (2020b), our results also show that VLFE activity in the region off Tokachi was the highest among the studied regions (Figure 9b). In contrast, shallow slow earthquake activity in other regions monitored via VLFEs were one order of magnitude less active than the shallow slow earthquake activity off Tokachi.

However, shallow slow earthquake monitoring via shallow tremors provides a different perspective (Figure 9c and 9d). The cumulative seismic moment released by shallow tremors is converted from the cumulative seismic energy radiation with a scaled energy of $3.0 \times 10^{-10}$. We note here that the completeness of the seismic energy count is insufficient because the tremor catalog constructed using the envelope correlation method detects only part of the entire tremor activity (Annoura et al., 2016). Tremor activity in the region off Tokachi had the largest seismic moment release among the studied regions. The cumulative seismic moment released over two years by shallow tremors is ~$2.5 \times 10^{17}$ Nm, which is comparable to the estimates obtained from shallow VLFEs. The regions off Iwate and Ibaraki also released seismic moments of ~$1.0 \times 10^{17}$ Nm, whereas the seismic moment released in these regions estimated from shallow VLFEs is one order of magnitude smaller. This difference is due to the differences in event-size distributions among the regions. Larger events occurred more dominantly in the region off Tokachi than in other regions along the Japan Trench (Figure 10). In the region off Tokachi, many large events occurred that were observed by onshore stations. However, the other regions contained many events that were too small to be observed by the onshore stations. Although the individual events were smaller, shorter recurrence intervals resulted in a large seismic moment released in these regions. Hence, shallow slow earthquake monitoring of shallow VLFEs that is based at onshore seismic stations could miss a significant amount of seismic moment released by small, but frequent, events. Monitoring small events is also important for understanding the source physics of slow earthquakes by analyzing, for example, event-size distributions (Nakano et al., 2019).

## 5. Conclusions

This study evaluated the seismicity of shallow slow earthquakes in the Nankai Trough and the Japan Trench in terms of the seismic energy rates of shallow tremors, the seismic moment rates of shallow VLFEs, and the scaled energies. We applied the method of Yabe et al. (2019), who estimated the seismic energy rate of shallow tremors in the DONET1 region of the Nankai Trough, to data from the DONET2 region in the Nankai trough and from S-net in the Japan Trench, with minor modifications. Site amplification of the OBSs and seismic attenuation due to a shallow prism were also estimated to conduct an accurate estimation of the seismic energy rates. The results indicate that the estimated site amplification is larger for the horizontal components than for the vertical components. Soft sediments on the seafloor contribute to large site amplification of the horizontal components. The strengths of the seismic attenuations are almost the same in the shallow prism at the Nankai Trough and at the Japan Trench. The estimated seismic energy rates of the shallow tremors ranged from $10^2$ to $10^5$ J/s, with spatial variations. Significant variations were observed in the northern Japan Trench, where shallow tremors exhibit belt-like distributions with small gaps near 40.7°N. Tremors in the region off Tokachi (northern section) had higher energy rates with long recurrence intervals, whereas those in the region off Iwate (southern section) had lower energy rates with short recurrence intervals. This correlation between the tremor sizes and recurrence intervals has also been observed for deep tremors. The seismic moment rate of the shallow VLFEs that accompany shallow tremors in the Japan Trench were also analyzed using onshore broadband seismic stations with Green's function developed using a three-dimensional seismic velocity model. Shallow VLFEs were detected in regions where the seismic energy rate of the shallow tremors is large. The scaled energy was estimated as approximately $10^{-9}$, although there were slight variations. Shallow slow earthquakes in the DONET1 region and the western cluster in the DONET2 region had higher scaled energy values ($10^{-9}$–$10^{-8}$), whereas shallow slow earthquakes in the eastern cluster in the

DONET 2 region and the Japan Trench had lower values ($10^{-10}$–$10^{-9}$), which is common for values estimated for deep slow earthquakes. We compared the cumulative seismic energies of the shallow tremors observed by the OBSs to those of the seismic moments of the shallow VLFEs observed by the onshore seismic stations, showing that the seismic moment release monitored via shallow VLFEs by far onshore seismic stations could be underestimated due to undetected small, but frequent, events that can be observed only as shallow tremors by OBSs.

## Acknowledgments

This research was supported by JSPS KAKENHI (Grant Nos. JP18K13639 and JP16H06477). We used the computer system at the Earthquake and Volcano Information Center, Earthquake Research Institute, University of Tokyo. The figures were partially produced using the GMT software package (Wessel et al., 2013). We would like to thank Editage (www.editage.com) for English language editing.

## Data Availability

Hi-net, F-net, S-net, and DONET2 data are available at the Hi-net website (https://doi.org/10.17598/NIED.0003; https://doi.org/10.17598/NIED.0005; https://doi.org/10.17598/NIED.0007; https://doi.org/10.17598/NIED.0008). DONET2 data prior to April 2016 are available to any reader directly upon a reasonable request to S. Y. Open SWPC software (Maeda et al., 2017) was downloaded from https://doi.org/10.5281/zenodo.3712649. The slow earthquake catalogs of Nakano et al. (2016, 2018) and Nishikawa et al. (2019) are available in the Slow Earthquake Database (http://www-solid.eps.s.u-tokyo.ac.jp/~sloweq/; Kano et al., 2018).

## Competing interests

The authors declare that they have no competing interests.

## References

Ando, M., 1975. Source mechanism and tectonic significance of historical earthquakes along the Nankai Trough, Japan. Tectonophysics, 27, 119–140. https://doi.org/10.1016/0040-1951(75)90102-X.

Ando, R., Takeda, N., Yamashita, T., 2012. Propagation dynamics of seismic and aseismic slip governed by fault heterogeneity and Newtonian rheology, J. Geophys. Res., 117, B11308. https://doi.org/10.1029/2012JB009532.

Annoura, S., Obara, K., Maeda, T., 2016. Total energy of deep low‐frequency tremor in the Nankai subduction zone, southwest Japan, Geophys. Res. Lett., 43, 2562– 2567. https://doi.org/10.1002/2016GL067780.

Aoi, S., Asano, Y., Kunugi, T., Kimura, T., Uehira, K., Takahashi, N., Ueda, H., Shiomi, K., Matsumoto, T., Fujiwara, H., 2020. MOWLAS: NIED observation network for earthquake, tsunami and volcano, Earth Planets Space, 72, 126. https://doi.org/10.1186/s40623-020-01250-x.

Araki, E., Saffer, D. M., Kopf, A. J., Wallace, L. M., Kimura, T., Machida, Y., Ide, S., Davis, E., IODP 365 shipboard scientists, 2017. Recurring and triggered slow-slip events near the trench at the Nankai trough subduction megathrust, Science, 356(6343) . https://doi.org/10.1126/science.aan3120.

Asano, Y., Obara, K., Ito, Y., 2008. Spatiotemporal distribution of very-low frequency earthquakes in Tokachi-oki near the junction of the Kuril and Japan trenches revealed by using array signal processing, Earth Planets Space, 60(8), 871 – 875. https://doi.org/10.1186/BF03352839.

Azuma, R., Hino, R., Ohta, Y., Ito, Y., Mochizuki, K., Uehira, K., Murai, Y., Sato, T., Takanami, T., Shinohara, M., Kanazawa, T., 2018. Along-arc heterogeneity of the seismic structure around a large coseismic shallow slip area of the 2011 Tohoku-oki earthquake: 2-D Vp structural estimation through an air gun-ocean bottom seismometer experiment in the Japan Trench subduction zone. J. Geophys. Res. Solid Earth, 123, 5249–5264. https://doi.org/10.1029/ 2017JB015361.

Baba, S., Takeo, A., Obara, K., Matsuzawa, T., Maeda, T., 2020a. Comprehensive detection of very low-frequency earthquakes off the Hokkaido and Tohoku Pacific coasts, northeastern Japan. J. Geophys. Res. Solid Earth, 125, e2019JB017988. https://doi.org/10.1029/2019JB017988.

Baba, S., Takemura, S., Obara, K., Noda, A., 2020b. Slow earthquakes illuminating interplate coupling heterogeneities in subduction zones. Geophys. Res. Lett., 47, e2020GL088089. https://doi.org/10.1029/2020GL088089.

Beroza, G. C., Ide, S., 2011. Slow Earthquakes and Nonvolcanic Tremor. Ann. Rev. Earth Planet. Sci., 39, 271-296. https://doi.org/10.1146/annurev-earth-040809-152531

Brudzinski, M. R., Allen, R. M., 2007. Segmentation in episodic tremor and slip all along Cascadia, Geology, 35(10), 907-910. https://doi.org/10.1130/G23740A.1.

DeMets. C., Gordon, R. G., Argus, D. F., Stein, S., 1994. Effect of recent revisions to the geomagnetic reversal time scale on estimate of current plate motions, Geophys. Res. Lett., 21(20), 2191-2194. https://doi.org/10.1029/94GL02118.

Dragert, H., Wang, K., James, T. S., 2001. A silent slip event on the deeper Cascadia subduction interface, Science, 292(5521), 1525–1528. https://doi.org/10.1126/science.1060152.

Fujie, G., Kodaira, S., Nakamura, Y., Morgan, J. P., Dannowski, A., Thorwart, M., Grevemeyer, I., Miura, S., 2020. Spatial variations of incoming sediments in the northeastern Japan arc and their implications for megathrust earthquakes: Geology, 48(6), 614-619. https://doi.org/10.1130/G46757.1.

Hasselmann, K., 1963. A Statistical Analysis of the Generation of Microseisms, Rev. Geophys., 1, 177–209. https://doi.org/10.1029/RG001i002p00177.

Hirano, N., Takahashi, E., Yamamoto, J., Abe, N., Ingle, S. P., Kaneoka, I., Hirata, T., Kimura, J., Ogawa, Y., Machida, S., Suyehiro, K., 2006. Volcanism in response to plate flexure, Science, 313, 1426–1428. https://doi.org/10.1126/science.1128235.

Hirose, F., Nakajima, J., Hasegawa, A., 2008. Three-dimensional seismic velocity structure and configuration of the Philippine Sea slab in southwestern Japan estimated by double-difference tomography, J. Geophys. Res., 113, B09315. https://doi.org/10.1029/2007JB005274.

Ide, S., 2016. Characteristics of slow earthquakes in the very low frequency band: Application to the Cascadia subduction zone. J. Geophys. Res. Solid Earth, 121, 5942–5952. https://doi.org/10.1002/2016JB013085.

Ide, S., Beroza, G. C., 2001. Does apparent stress vary with earthquake size?, Geophys. Res. Lett., 28(171), 3349–3352. https://doi.org/10.1029/2001GL013106.

Ide, S., Yabe, S., 2014. Universality of slow earthquakes in the very low frequency band, Geophys. Res. Lett., 41, 2786–2793. https://doi.org/10.1002/2014GL059712.

Ide, S., Maury, J., 2018. Seismic moment, seismic energy, and source duration of slow earthquakes: Application of the Brownian slow earthquake model to three major subduction zones. Geophys. Res. Lett., 45, 3059– 3067. https://doi.org/10.1002/2018GL077461.

Idehara, K., Yabe, S., Ide, S., 2014. Regional and global variations in the temporal clustering of tectonic tremor activity, Earth Planets Space, 66, 66. https://doi.org/10.1186/1880-5981-66-66.

Ike, T., Moore, G.F., Kuramoto, S., Park, J. ‐ O., Kaneda, Y., Taira, A., 2008. Variations in sediment thickness and type along the northern Philippine Sea Plate at the Nankai Trough. Island Arc, 17: 342-357. https://doi.org/10.1111/j.1440-1738.2008.00624.x

Ito, Y., Obara, K., Shiomi, K., Sekine, S., Hirose, H., 2007. Slow earthquakes coincident with episodic tremors and slow slip events, Science, 315(5811), 503-506. https://doi.org/10.1126/science.1134454.

Ito, Y., Asano, Y., Obara, K., 2009. Very ‐ low ‐ frequency earthquakes indicate a transpressional stress regime in the Nankai accretionary prism, Geophys. Res. Lett., 36, L20309. https://doi.org/10.1029/2009GL039332.

Ito, Y., Hino, R., Kido, M., Fujimoto, H., Osada, Y., Inazu, D., Ohta, Y., Iinuma, T., Ohzono, M., Miura, S., Mishina, M., Suzuki, K., Tsuji, T., Ahi, J., 2013. Episodic slow slip events in the Japan subduction zone before the 2011 Tohoku-Oki earthquake, Tectonophysics, 600, 14-26. https://doi.org/10.1016/j.tecto.2012.08.022.

Ito, Y., Hino, R., Suzuki, S., Kaneda, Y., 2015. Episodic tremor and slip near the Japan Trench prior to the 2011 Tohoku ‐ Oki earthquake. Geophys. Res. Lett., 42, 1725– 1731. https://doi.org/10.1002/2014GL062986.

Kaneda, Y., Kawaguchi, K., Araki, E., Matsumoto, H., Nakamura, T., Kamiya, S., Ariyoshi, K., Hori, T., Baba, T., Takahashi, N., 2015. Development and application of an advanced ocean floor network system for megathrust earthquakes and tsunamis. In: Favali P et al. (eds) Seafloor observatories. Springer, Berlin, pp 643–662. https://doi.org/10.1007/978-3-642-11374-1_25.

Kaneko, L., Ide, S., Nakano, M., 2018. Slow earthquakes in the microseism frequency band (0.1.1.0 Hz) off Kii Peninsula, Japan, Geophysical Research Letters, 45, 2618– 2624. https://doi.org/10.1002/2017GL076773.

Kano, M., Aso, N., Matsuzawa, T., Ide, S., Annoura, S., Arai, R., Baba, S., Bostock, M., Chao, K., Heki, K., Itaba, S., Ito, Y., Kamaya, N., Maeda, T., Maury, J., Nakamura, M., Nishimura, T., Obana, K., Ohta, K., Poiata, N., Rousset, B., Sugioka, H., Takagi, R., Takahashi, T., Takeo, A., Tu, Y., Uchida, N., Yamashita, Y., Obara, K., 2018. Development of a Slow Earthquake Database, Seismol. Res. Lett., 89 (4), 1566-1575. https://doi.org/10.1785/0220180021.

Kawaguchi, K., Kaneko, S., Nishida, T., Komine, T., 2015. Construction of the DONET real-time sea floor observatory for earthquakes and tsunami monitoring. In: Favali P et al. (eds) Seafloor observatories. Springer, Berlin, pp 211–228. https://doi.org/10.1007/978-3-642-11374-1_10.

Kodaira, S., Nakamura, Y., Yamamoto, Y., Obana, K., Fujie, G., No, T., Kaiho, Y., Sato, T., Miura, S., 2017. Depth-varying structural characteristics in the rupture zone of the 2011 Tohoku-oki earthquake: Geosphere, 13(5), 1408–1424. https://doi.org/10.1130/GES01489.1.

Koketsu, K., Miyake, H., Suzuki, H., 2012. Japan integrated velocity structure model version 1. Proceedings of the 15th World Conference on Earthquake Engineering, 1–4.

Li, C., Hao, H., Li, H., Bi, K., 2015. Theoretical modeling and numerical simulation of seismic motions at seafloor, Soil Dyn. Earthq. Eng., 77, 220-225. https://doi.org/10.1016/j.soildyn.2015.05.016.

Longuet-Higgins, M. S., 1950. A Theory of the Origin of Microseisms, Philos. Trans. R. Soc. London, Ser. A, 243, 1–35. https://doi.org/10.1098/rsta.1950.0012.

Maeda, T., Obara, K., 2009. Spatiotemporal distribution of seismic energy radiation from low-frequency tremor in western Shikoku, Japan, J. Geophys. Res., 114, B00A09. https://doi.org/10.1029/2008JB006043.

Maeda, T., Takemura, S., Furumura, T., 2017. OpenSWPC: An open-source integrated parallel simulation code for modeling seismic wave propagation in 3D heterogeneous viscoelastic media. Earth, Planets Space, 69(1), 1–20. https://doi.org/10.1186/s40623‐017‐0687‐2.

Masuda, K., Ide, S., Ohta, K., Matsuzawa, T., 2020. Bridging the gap between low-frequency and very-low-frequency earthquakes, Earth Planets Space, 72:47. https://doi.org/10.1186/s40623-020-01172-8.

Matsuzawa, T., Asano, Y., Obara, K., 2015. Very low frequency earthquakes off the Pacific coast of Tohoku, Japan. Geophys. Res. Lett., 42, 4318– 4325. https://doi.org/10.1002/2015GL063959.

Maury, J., Ide, S., Cruz ‐ Atienza, V. M., Kostoglodov, V., Gonzáles ‐ Molina, G., Péres ‐ Campos, X., 2016. Comparative study of tectonic tremor locations: Characterization of slow earthquakes in Guerrero, Mexico. J. Geophys. Res. Solid Earth, 121, 5136–5151. https://doi.org/10.1002/2016JB013027

Maury, J., Ide, S., Cruz ‐ Atienza, V. M., Kostoglodov, V., 2018. Spatiotemporal variations in slow earthquakes along the Mexican subduction zone J. Geophys. Res. Solid Earth, 123, 1559–1575. https://doi.org/10.1002/2017JB014690.

Nagai, R., Kikuchi, M., Yamanaka, Y., 2001. Comparative study on the source processes of recurrent large earthquakes in the Sanriku ‐ oki region: The 1968 Tokachi ‐ oki earthquake and the 1994 Sanriku ‐ oki earthquake. Zishin Journal of the Seismological Society of Japan, 54(2), 267–280. (in Japanese)

Nakamura, Y., Kodaira, S., Cook, B.J., Jeppson, T., Kasaya, T., Yamamoto, Y., Hashimoto, Y., Yamaguchi, M., Obana, K., Fujie, G., 2014. Seismic imaging and velocity structure around the JFAST drill site in the Japan Trench: low V p, high V p/V s in the transparent frontal prism. Earth Planets Space 66, 121. https://doi.org/10.1186/1880-5981-66-121.

Nakano, M., Hori, T., Araki, E., Takahashi, N. Kodaira S., 2016. Ocean floor networks capture low-frequency earthquake events. EOS. https://doi.org/10.1029/2016EO052877.

Nakano, M., Hori, T., Araki, E., Kodaira, S., Ide, S., 2018. Shallow very-low-frequency earthquakes accompanied by slow slip events, Nankai Trough, Japan. Nature Comms., 9, 984. https://doi.org/10.1038/s41467-018-03431-5.

Nakano, M., Yabe, S., Sugioka, H., Shinohara, M., Ide, S., 2019. Event size distribution of shallow tectonic tremors in the Nankai trough. Geophys. Res. Lett., 46, 5828– 5836. https://doi.org/10.1029/2019GL083029.

National Research Institute for Earth Science and Disaster Resilience (2019a), NIED DONET, National Research Institute for Earth Science and Disaster Resilience. https://doi.org/10.17598/NIED.0008.

National Research Institute for Earth Science and Disaster Resilience (2019b), NIED Hi-net, National Research Institute for Earth Science and Disaster Resilience. https://doi.org/10.17598/NIED.0003.

National Research Institute for Earth Science and Disaster Resilience (2019c), NIED F-net, National Research Institute for Earth Science and Disaster Resilienc. https://doi.org/.17598/NIED.0005.

National Research Institute for Earth Science and Disaster Resilience (2019d), NIED S-net, National Research Institute for Earth Science and Disaster Resilience. https://doi.org/10.17598/NIED.0007.

Nishikawa, T., Matsuzawa, T., Ohta, K., Uchida, N., Nishimura, T. Ide, S., 2019. The slow earthquake spectrum in the Japan Trench illuminated by the S-net seafloor observatories. Science, 365(6455), 808–813. https://doi.org/10.1126/science.aax5618.

Obara, K., 2002. Nonvolcanic deep tremor associated with subduction in southwest Japan, Science, 296(5573), 1679–1681. https://doi.org/10.1126/science.1070378.

Obara, K., 2011. Characteristics and interactions between non-volcanic tremor and related slow earthquakes in the Nankai subduction zone in southwest Japan. J. Geodynamics, 52, 3-4, 229-248. https://doi.org/10.1016/j.jog.2011.04.002.

Obara, K., Ito, Y., 2005. Very low-frequency earthquake excited by the 2004 off the Kii peninsula earthquake: A dynamic deformation process in the large accretionary prism, Earth Planets Space, 57, 321–326. https://doi.org/10.1186/BF03352570.

Obara, K., Kato, A., 2016. Connecting slow earthquakes to large earthquakes Science, 353(6296), 253-257. https://doi.org/10.1126/science.aaf1512.

Obara, K., Hirose, H., Yamamizu, F., Kasahara, K., 2004. Episodic slow slip events accompanied by non-volcanic tremors in the southwest Japan subduction zone, Geophys. Res. Lett., 31, L23602. https://doi.org/10.1029/2004GL020848.

Phillips, N. J., Motohashi, G., Ujiie, K., Rowe, C. D., 2020. Evidence of localized failure along altered basaltic blocks in tectonic mélange at the updip limit of the seismogenic zone: Implications for the shallow slow earthquake source. Geochem. Geophys. Geosys., 21, e2019GC008839. https://doi.org/10.1029/2019GC008839

Rogers, G., Dragert, H., 2003. Episodic tremor and slip on the Cascadia subduction zone: The chatter of silent slip, Science, 300(5627), 1942–1943. https://doi.org/10.1126/science.1084783.

Smith, W. H. F., Sandwell, D. T., 1997. Global seafloor topography from satellite altimetry and ship depth soundings, Science, 277, 1957-1962. https://doi.org/10.1126/science.277.5334.1956.

Takemoto, T., Furumura, T., Saito, T., Maeda, T., Noguchi, S., 2012. Spatial- and frequency-dependent properties of site amplification factors in Japan derived by the Coda Normalization Method, Bull. Seismol. Soc. Am., 102(4), 1462-1476. https://doi.org/10.1785/0120110188.

Takemura, S., Matsuzawa, T., Noda, A., Tonegawa, T., Asano, Y., Kimura, T. Shiomi, K., 2019. Structural characteristics of the Nankai Trough shallow plate boundary inferred from shallow very low frequency earthquakes. Geophys. Res. Lett., 46. https://doi.org/10.1029/2019GL082448.

Takemura, S., Yabe, S., Emoto, K., 2020. Modeling high-frequency seismograms at ocean bottom seismometers: effects of heterogeneous structures on source parameter estimation for small offshore earthquakes and shallow low-frequency tremors, Geophys. J. Int., accepted. https://doi.org/10.1093/gji/ggaa404.

Tanaka, S., Matsuzawa, T., Asano, Y., 2019. Shallow low‐frequency tremor in the northern Japan Trench subduction zone Geophys. Res. Lett., 46, 5217– 5224. https://doi.org/.1029/2019GL082817.

Tonegawa, T., Araki, E., Kimura, T., Nakamura, T., Nakano, M., Suzuki, K., 2017. Sporadic low-velocity volumes spatially correlate with shallow very low frequency earthquake clusters, Nature Comms., 8, 2048, doi: 10.1038/s41467-017-02276-8.

Tsuru, T., Park, J., Miura, S., Kodaira, S., Kido, Y. Hayashi, T., 2002. Along-arc structural variation of the plate boundary at the Japan Trench margin: Implications of interplate coupling. J. Geophys. Res., 107(B12), 2357. https://doi.org/10.1029/ 2001JB001664.

Tsuru, T., Park, J., Takahashi, N., Kodaira, S., Kido, Y., Kaneda, Y., Kono, Y., 2000. Tectonic features of the Japan Trench convergent margin off Sanriku, northeastern Japan, revealed by multichannel seismic reflection data. J. Geophys. Res., 105(B7), 16,403–16,413. https://doi.org/10.1029/2000JB900132.

Ujiie, K., Saishu, H., Fagereng, A., Nishiyama, N., Otsubo, M., Masuyama, H., Kagi, H., 2018. An explanation of episodic tremor and slow slip constrained by crack-seal veins and viscous shear in subduction mélange. Geophys. Res. Lett. 45, 5371– 5379. https://doi.org/10.1029/2018GL078374.

Wech, A., Creager, K., 2011. A continuum of stress, strength, and slip in the Cascadia subduction zone. Nature Geosci., 4, 624–628. https://doi.org/10.1038/ngeo1215.

Wessel, P., Smith, W. F., Scharroo, R., Luis, J., Wobbe, F., 2013. Generic Mapping Tools: Improved Version Released, EOS, Transactions, Am. Geophys. Un., 94 (45), 409. https://doi.org/10.1002/2013EO450001.

Yamamoto, Y., Obana, K., Kodaira, S., Hino, R., Shinohara, M., 2014. Structural heterogeneities around the megathrust zone of the 2011 Tohoku earthquake from tomographic inversion of onshore and offshore seismic observations, J. Geophys. Res. Solid Earth, 119, 1165–1180. https://doi.org/10.1002/2013JB010582.

Yokota, Y., Ishikawa, T., Watanabe, S., Tashiro, T., Asada, A., 2016. Seafloor geodetic constraints on interplate coupling of the Nankai Trough megathrust zone. Nature, 534, 374–377. https://doi.org/10.1038/nature17632.

**Figures and Tables**

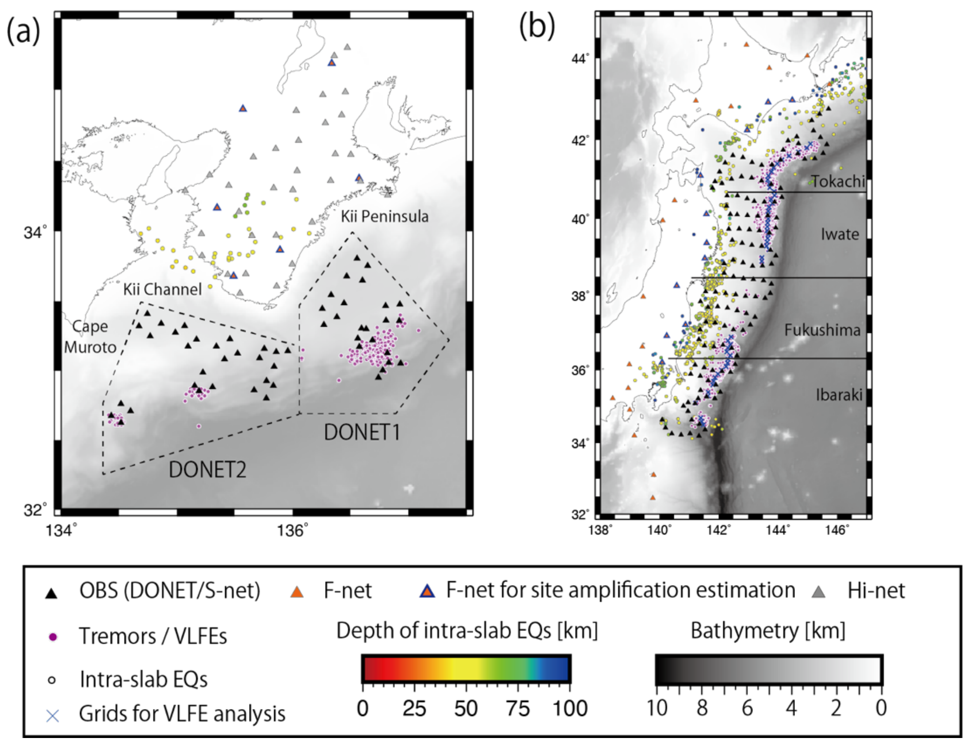


Figure 1. Regional map of the (a) Nankai Trough and (b) the Japan Trench. Black, orange, and gray triangles represent ocean bottom seismometers (OBSs) (DONET stations in the Nankai Trough and S-net stations in the Japan Trench), F-net stations, and Hi-net stations respectively. F-net stations with blue edges are stations that were used for site amplification analyses. Purple circles indicate the hypocenters of VLFEs in the Nankai Trough (Nakano et al., 2016, 2018) and tremors in the Japan Trench (Nishikawa et al., 2019). Other circles indicate the hypocenters of intra-slab earthquakes in the JMA catalog. Colors of circles for intra-slab earthquakes indicate their depths. Blue crosses are grids set for the VLFE analyses explained in Section 2.3. Background gray scale denotes the bathymetry (Smith and Sandwell, 1997). In the Nankai Trough, the DONET1 region denoted by dashed lines was investigated by Yabe et al. (2019).

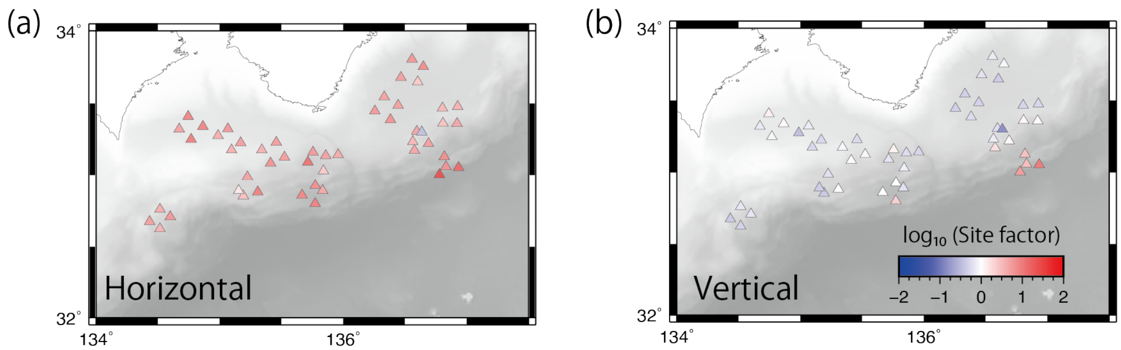


Figure 2. Estimated site factors of the DONET stations for (a) horizontal and (b) vertical components.

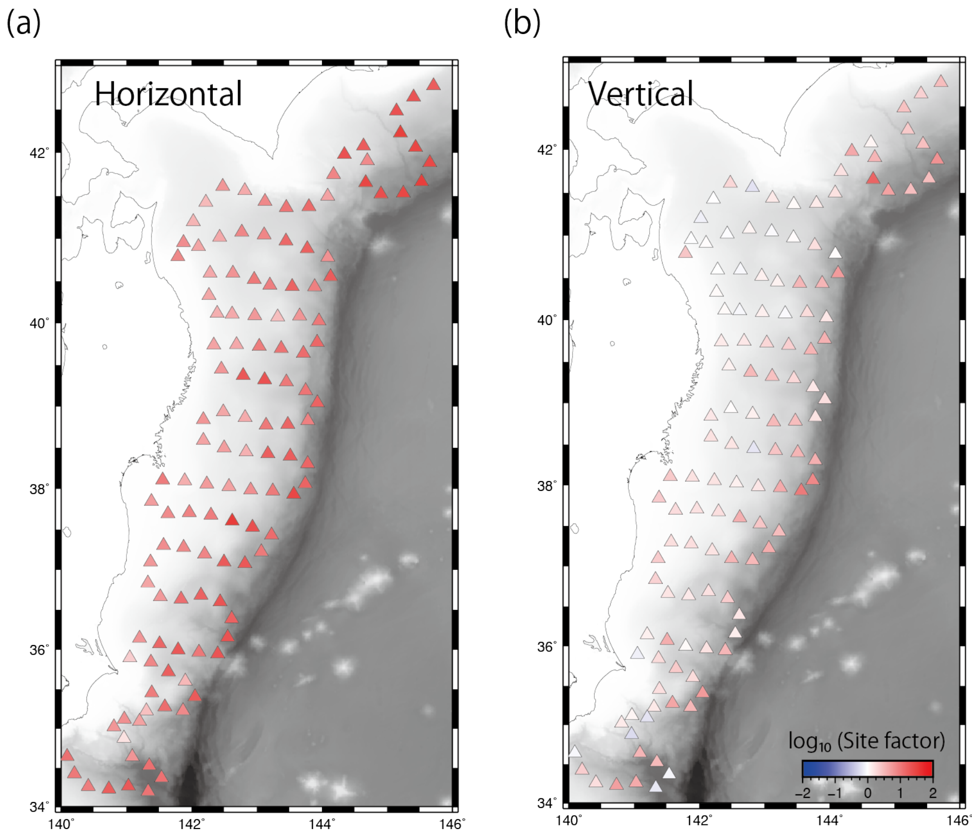


Figure 3. Estimated site factors of the S-net stations for (a) horizontal and (b) vertical components.

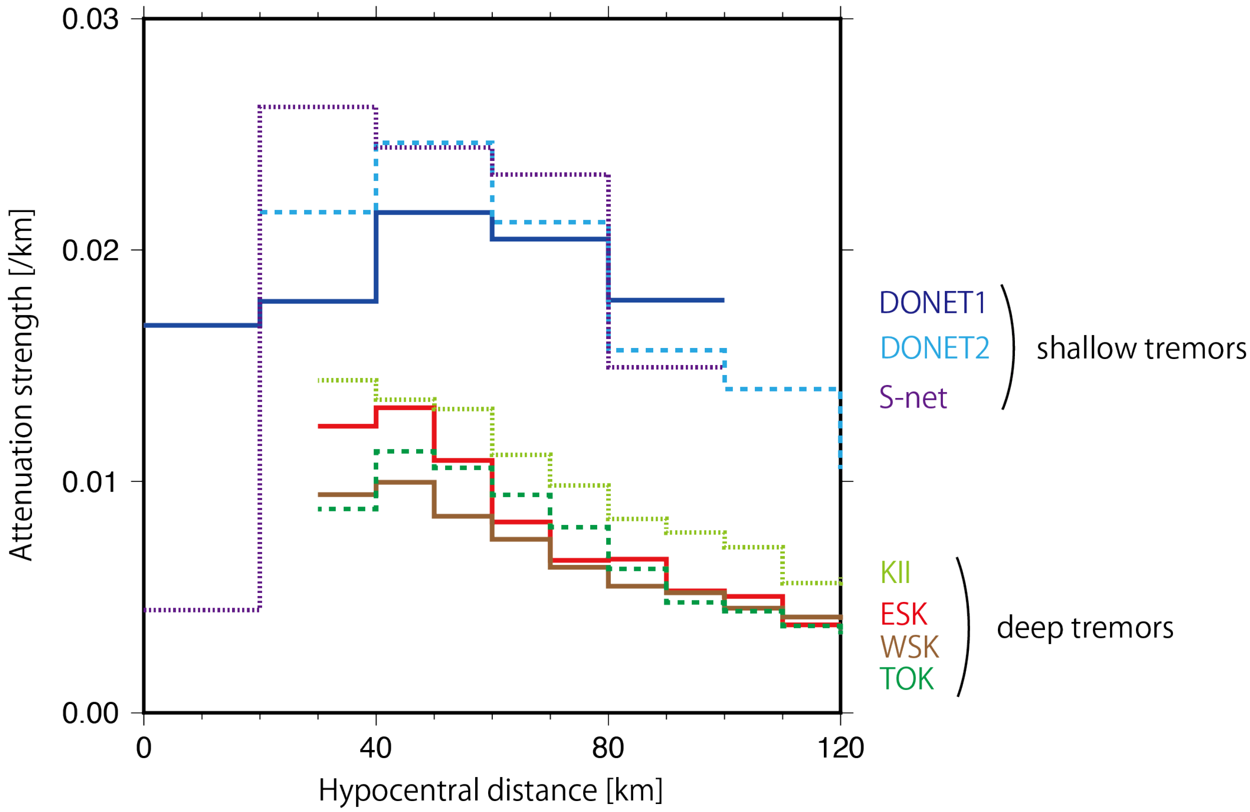


Figure 4. Estimated seismic attenuation relative to hypocentral distance. Results from DONET1 (blue; Yabe et al., 2019), DONET2 (light blue; this study), and S-net (purple; this study) stations are presented, as well as those from the western Shikoku (WSK; brown), eastern Shikoku (ESK; red), Kii (KII; light green), and Tokai (TOK; green) regions estimated with deep tremors (Yabe & Ide, 2014).

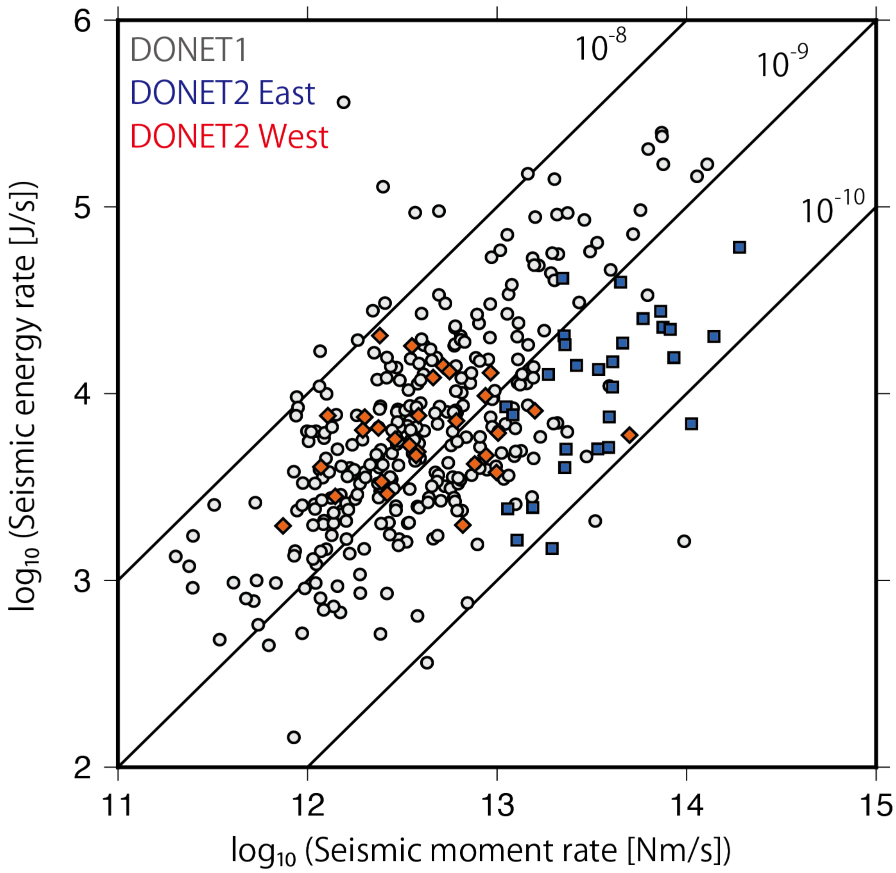


Figure 5. Estimated source parameters in the Nankai Trough. Colors of the circles indicate the tremor locations: gray circles for the DONET1 region (from Yabe et al., 2019), blue squares for the eastern cluster in the DONET2 region, and red diamonds for the western cluster in the DONET2 region). Black lines indicate constant scaled energies of $10^{-8}$, $10^{-9}$, and $10^{-10}$.

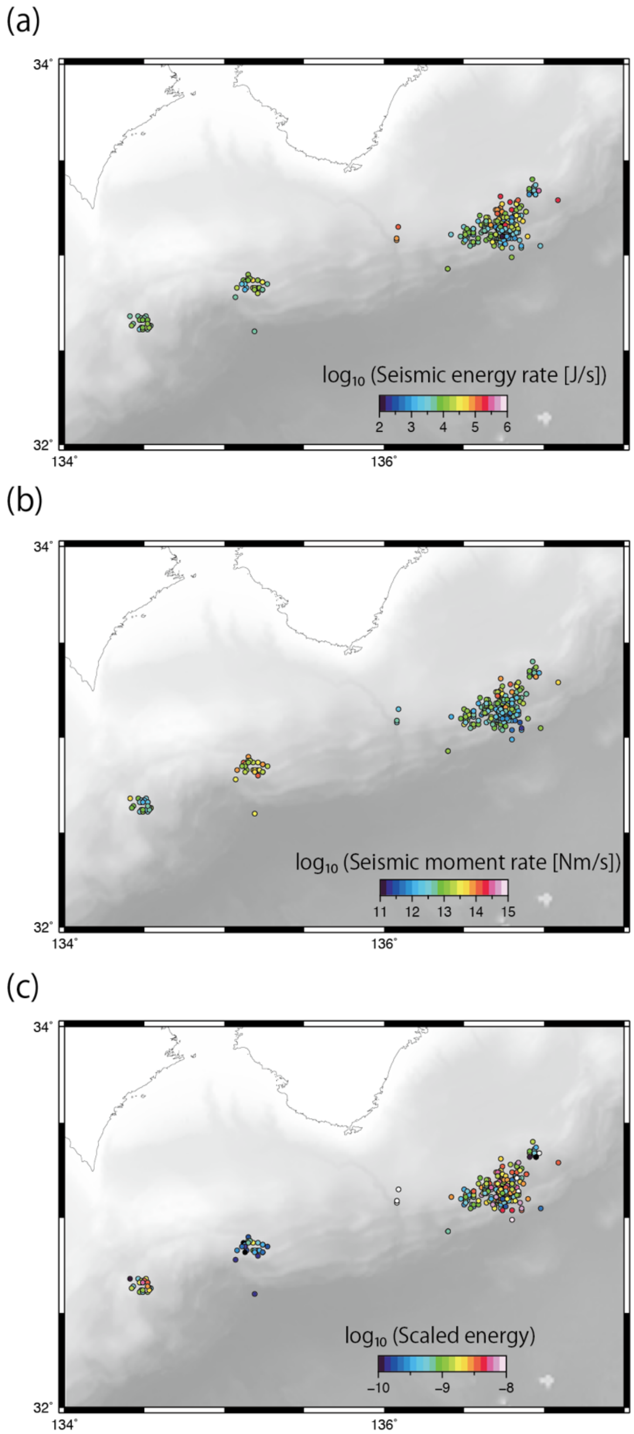


Figure 6. Spatial distributions of estimated seismic source parameters in the Nankai Trough. (a) Seismic energy rate, (b) seismic moment rate, and (c) scaled energy. Results from Yabe et al. (2019) are also included for the DONET1 region.

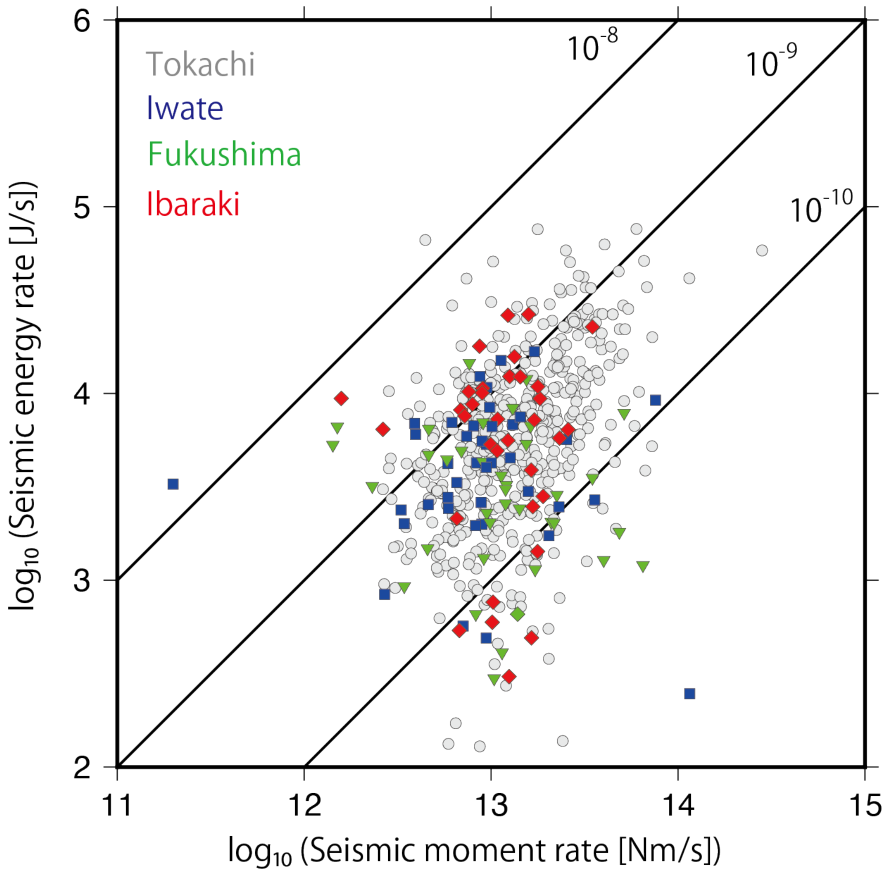


Figure 7. Estimated source parameters in the Japan trench. Colors of the circles indicate the tremor locations: gray circles for the region off Tokachi, blue squares for the region off Iwate, green triangles for the region off Fukushima, and red diamonds for the region off Ibaraki). Black lines indicate constant scaled energies of $10^{-8}$, $10^{-9}$, and $10^{-10}$.

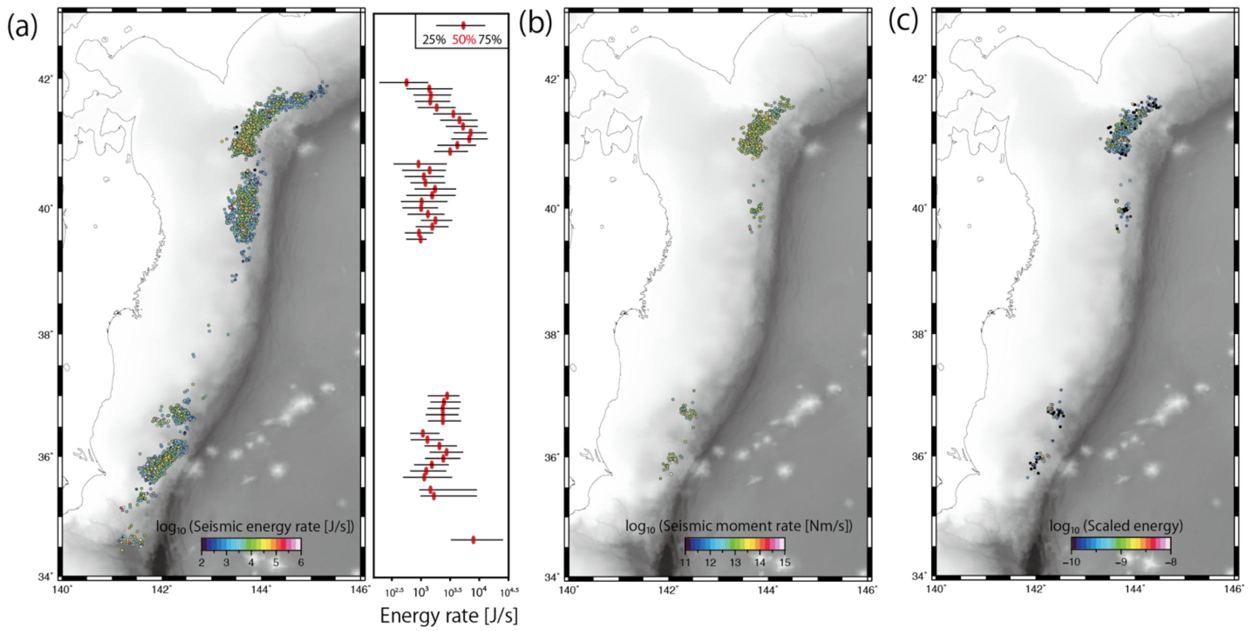


Figure 8. Spatial distributions of the estimated seismic source parameters in the Japan Trench. (a) Seismic energy rate, (b) seismic moment rate, and (c) scaled energy. The right panel in (a) shows the 25th, 50th, and 75th percentiles of the energy rate for each bin in the latitude direction (0.2° bin size).

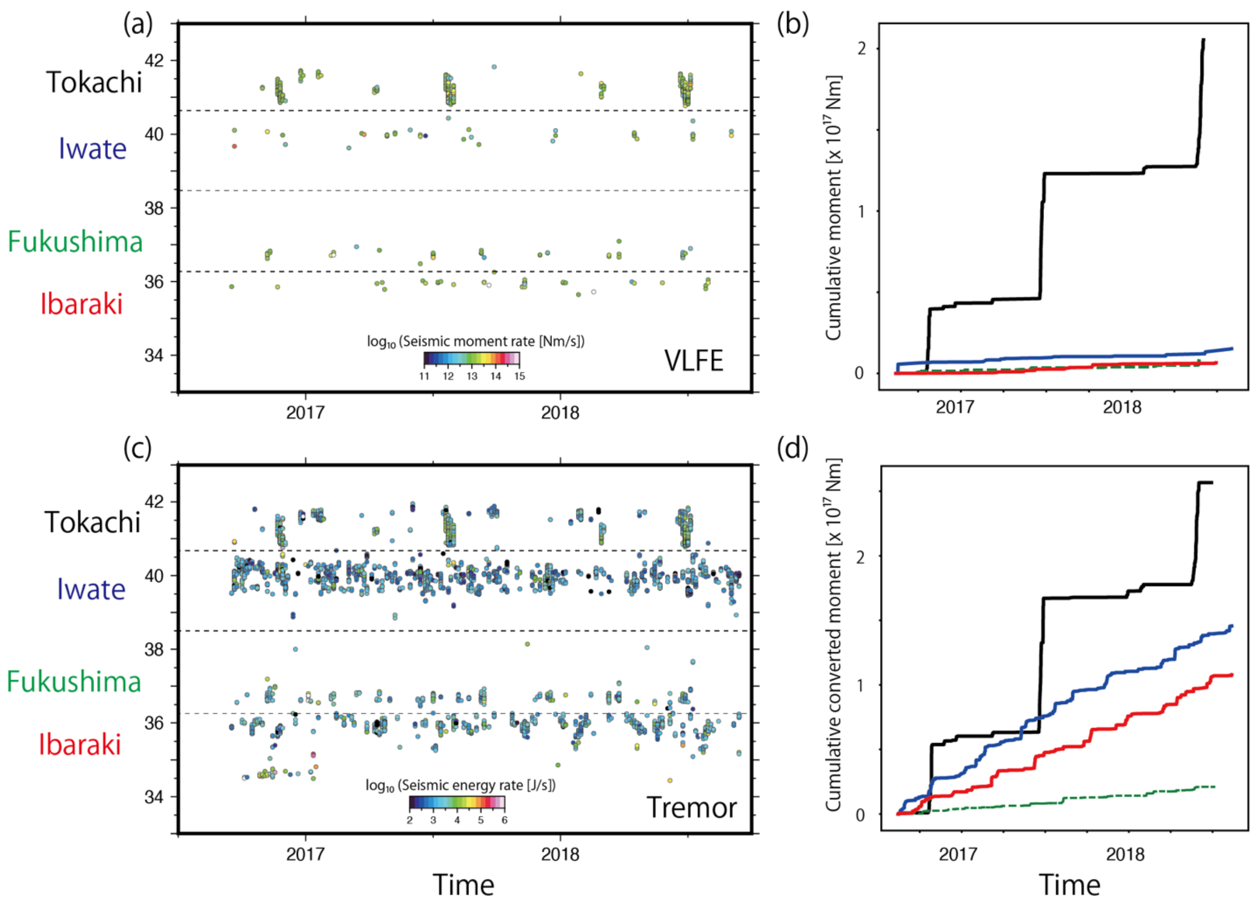


Figure 9. Time plots of seismic energy and seismic moment rates in the Japan Trench. (a) Time plots of the seismic moment rates estimated for shallow tremors. (b) Time plots of the cumulative moment rates for VLFEs. Colors of the lines represent regions: black for the region off Tokachi, blue for the region off Iwate, green dashed line for the region off Fukushima, and red for the region off Ibaraki. (c) Time plots of seismic energy rates for shallow tremors. (d) Time plots of the cumulative moment rates for tremors, which have been converted from the estimated energies using a scaled energy of 3.0 x $10^{-10}$.

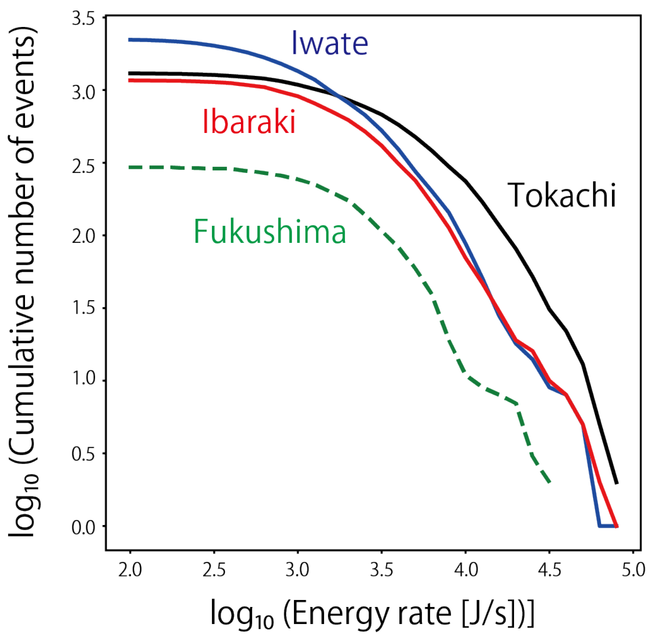


Figure 10. The event-size distributions of shallow tremors in the four regions of the Japan Trench. Black indicates the region off Tokachi, blue indicates the region off Iwate, green dashed line the region off Fukushima, and red indicates the region off Ibaraki.

Table 1. Summary of seismic energy rates and recurrence intervals of shallow tremors in the Japan Trench.

| Region | Recurrence intervals | Median energy rate | Scaled energy |
|---|---|---|---|
| Tokachi | 0.5–1 year | 1700 J/s | $10^{-10}$–$10^{-9}$ |
| Iwate | 1–2 months | 830 J/s | $10^{-10}$–$10^{-9}$ |
| Fukushima | ~3 months | 1350 J/s | $10^{-10}$–$10^{-9}$ |
| Ibaraki | ~3 months | 1470 J/s | $10^{-10}$–$10^{-9}$ |